

Mechanical characterization of biomimetic membranes by micro-shaft poking

Mark Ahearne, Eleftherios Siamantouras, Ying Yang and Kuo-Kang Liu

J. R. Soc. Interface 2009 **6**, 471-478 first published online 26 August 2008
doi: 10.1098/rsif.2008.0317

References

[This article cites 19 articles, 2 of which can be accessed free](#)

<http://rsif.royalsocietypublishing.org/content/6/34/471.full.html#ref-list-1>

Subject collections

Articles on similar topics can be found in the following collections

[nanotechnology](#) (19 articles)

[bioengineering](#) (17 articles)

[biomaterials](#) (28 articles)

Email alerting service

Receive free email alerts when new articles cite this article - sign up in the box at the top right-hand corner of the article or click [here](#)

To subscribe to *J. R. Soc. Interface* go to: <http://rsif.royalsocietypublishing.org/subscriptions>

Mechanical characterization of biomimetic membranes by micro-shaft poking

Mark Ahearne, Eleftherios Siamantouras, Ying Yang and Kuo-Kang Liu*

Institute of Science and Technology in Medicine, Keele University, Stoke-on-Trent ST4 7QB, UK

The popularity of biomimetic membranes has recently increased due to their biomedical applications such as tissue engineering/regenerative medicine and biosensors. Characterization of the viscoelastic properties of these membranes is important in developing functional membranes. A new micro-shaft poking technique has been developed, which is free from the complication of substrate backing, and which is normally an intractable problem in conventional indentation testing of membrane materials. A tailored indentation apparatus with a spherical indenter and a force resolution and displacement of 1 μ N and 1 μ m was constructed. Alginate and agarose were used to fabricate biomimetic membranes. Chicken epidermis was examined to represent a real biological tissue. The results show that the elastic modulus increased with concentration in hydrogels. Epidermis moduli appeared to increase with increased strain. Stress relaxation tests have also been conducted to examine the time-dependent behaviours of various hydrogels and a viscoelastic model has been correspondingly developed and applied to describe the experimental results. Potential applications of this new instrument to other membranes, both artificial and biological, have also been addressed.

Keywords: instrumentation; hydrogel; mechanical characterization; microengineering; biological tissue

1. INTRODUCTION

Biomimetic materials have been under investigation for use in tissue regeneration and the construction of the next generation of biomedical devices, including the development of engineered tissues and designing cell-based biosensors. The viscoelastic and mechanical properties of these membranes play an important role in their performance and durability and ultimately dictate whether the applications are successful or not. Therefore, there is a great need for the development of new techniques for mechanically characterizing these emerging biomimetic materials such as hydrogels (Callister 1994; Ratner *et al.* 1996). Mechanical characterization of real biological tissue is also essential to allow membranes that interface with tissues and tissue engineered constructs to be developed with appropriate mechanical strength. However, the fragility and viscoelasticity of these materials make their mechanical characterization in a quantitative manner highly challenging.

Despite the difficulty in experimentally measuring the mechanical properties of soft biological materials, recent progress in the development of new instrumentation has made microscale characterization more feasible (Lu *et al.* 2004). Several different mechanical testing techniques that were developed for mechanically testing biological materials have been described in depth previously (Ahearne *et al.* 2005). The common

fundamental principle among these methods is to determine the material deformation under an applied load without destruction of the specimens. Among these, bulge or blister testing, nanoindentation, and microtensile testing are prevailingly used for mechanical characterization of soft biomimetic materials (Liu & Ju 2001; Espinosa *et al.* 2003; Liu *et al.* 2004). Testing via bulging or nanoindentation alleviates many of the problems such as mounting of the specimen and providing sufficient resolution of measurements (Scott *et al.* 2004). Moreover, the data measured by using different testing techniques are often scattered. Such variations have been recognized to be attributed to the technological means employed by each technique and the calibration. Also, the different requirements for conducting the experiments and interpretation of results will also contribute to the discrepancy (Menciassi *et al.* 2001; Khoo 2003). Therefore, the mechanical properties of the soft materials are difficult to be unequivocally determined when the various techniques are compared (Espinosa *et al.* 2003).

In this work, a new ultra-precise measuring instrument, micro-shaft poking (MSP), for characterizing mechanical properties of biomimetic materials is described. Based on simultaneous force–displacement measurements, the elastic modulus of soft membranes can be determined. This instrument provides a broad range of measurements to facilitate large deformation analysis as well as time-dependent force measurements, with microscale resolution. The characterization of circular biomimetic hydrogel membranes and animal

*Author for correspondence (i.k.liu@keele.ac.uk).

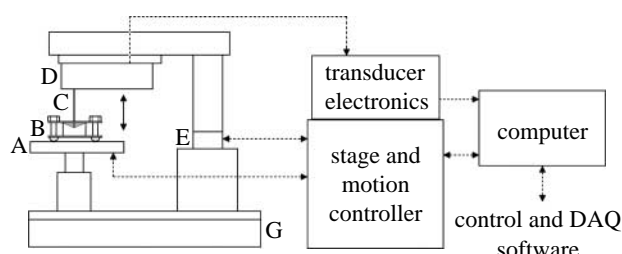


Figure 1. Schematic of the instrumental set-up: (A) *xy* translation stage; (B) membrane holder; (C) spherical tip; (D) force transducer; (E) microstepping motorized actuator; (G) anti-vibration table.

skin whose properties are of great interest for biomedical applications has been examined. The successful correlation of our results validated the performance of the newly developed system.

2. EXPERIMENTAL SET-UP

2.1. Instrumental set-up

The newly developed instrument for measuring force as a function of displacement was constructed as shown schematically in figure 1. The system is based around an inverted optical microscope (Eclipse TE 2000S, Nikon, USA), incorporated with an *xyz* motorized motion control interfaced with an external PC. The microscope's *z*-axis motorized stage, which is capable of 1 μm steps and a travelling distance of up to 8.5 mm, was used as a displacement actuator (ESP300, Newport, Irvine, CA). A force transducer (404A, Aurora Scientific, Inc., Canada) was firmly mounted to a specially designed solid arm attached to the *z*-axis stage. The force transducer had a force resolution of 1 μN and could measure forces up to 100 mN. The stability of the solid arm prevents the 'dead' weight effect of the transducer's head in the output signal and helps to avoid bending of the interior housing of the transducer, which might offset the output. In addition, it ensures precise loading in a vertical position. In its final form, the instrumental set-up has a force and displacement resolution of 1 μN and 1 μm , respectively.

A fine spherical tip of diameter 380 μm was attached at the end of the force transducer's output tube to allow deformation of samples. A sample holder was designed to facilitate mounting of a circular membrane between a thin steel plate and cylindrical plastic tube as shown in figure 2. The holes in the plate and the cylindrical tube had the same inner diameter (11 mm). The position of the membrane for central alignment could be adjusted precisely by tuning a two-dimensional (*x*-*y*) translation stage (ASSY STAGE 25, Cell Robotics, Inc., USA), with a resolution higher than 2 μm . A transparent plastic sheet marked with a central alignment sign was used for precisely positioning the spherical indenter to the centre of the membrane prior to each experiment. The samples were deformed at a rate of 25 $\mu\text{m s}^{-1}$. The force transducer signal was filtered and amplified by using differential amplification (S 400A, Aurora Scientific, Inc.). The amplified analogue signal was transmitted through a connector

block (DAQ SCB-68, National Instruments, USA) into a data acquisition (DAQ) board (PCI DAQ-6036E, National Instruments) for digitization and further processing. The acquired data were displayed and recorded by a tailored software design based on the LABVIEW platform (National Instruments).

2.2. Material preparation

Two types of hydrogel membranes, alginate and agarose, were fabricated as previously described (Ahearne *et al.* 2005). A 2 per cent (w/v) solution of sodium alginate was formed by dissolving 2 g of Protanal LF200 S (FMC BioPolymer, Norway) in 100 ml of deionized water using a magnetic stirrer. Several different concentrations of the alginate solution were formed by adjusting the ratio of alginate powder to deionized water. When fully dissolved the alginate was sterilized via autoclave. Filter paper rings (Millipore, USA) of inner diameter 11 mm and outer diameter of approximately 15 mm were placed on the bottom of small Petri dishes. These rings reduced the amount of shrinkage of the hydrogel after cross linking and allowed the hydrogels to be lifted from the Petri dishes. Two hundred microlitres of alginate solution were poured inside and over each ring. Five millilitres of 0.5 M filtered calcium chloride solution (CaCl_2) were added over the alginate. The application of CaCl_2 caused the sodium in the alginate to be replaced by calcium, which resulted in cross-linking and formation of a hydrogel. Once applied, the CaCl_2 solution had to cover the alginate quickly to prevent the hydrogel from forming unevenly. After 10 min, the CaCl_2 solution was removed and the hydrogel was washed twice in phosphate buffered saline (PBS; Sigma, UK).

Agarose hydrogels were made using agarose type 1 (Sigma). A 2 per cent (w/v) agarose solution was produced by dissolving 0.2 g of agarose powder in 10 ml PBS. For lower concentrations, less agarose powder was required. The powder was dissolved by heating the solution to over 60°C. When fully dissolved, the solution was filtered to remove any impurities. Two hundred microlitres of the solution were applied to Petri dishes with circular filter paper rings as described previously. The hydrogels were formed by cooling at room temperature. Once the hydrogel had formed, water or PBS was added to the Petri dish to prevent the agarose from dehydrating.

In addition to hydrogel membranes, the mechanical characteristics of chicken epidermis were examined to demonstrate this system's ability to measure soft biological tissues. The epidermal layer of skin was removed from the back of fresh chickens. The epidermis was cut into circular sections greater than 11 mm in diameter. The sections were stored in water at 4°C until ready for measurement.

2.3. Statistical analysis

Statistical analysis of Young's moduli was performed using one-way ANOVA Tukey's test with a 95% confidence interval ($n=4$). Nonlinear regression analysis was used to model stress relaxation data.

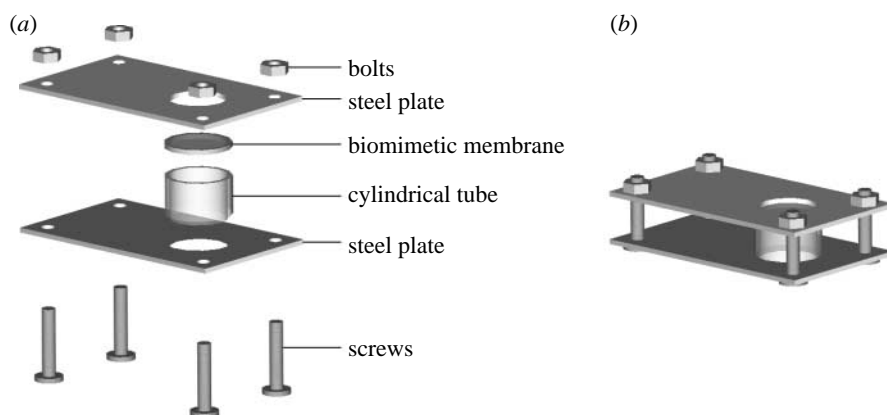


Figure 2. Biomimetic membrane holder: (a) disassembled and (b) fully assembled.

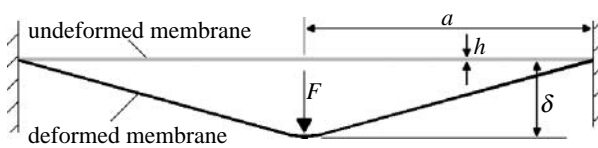


Figure 3. Schematic of the indentation of a hydrogel by the MSP.

3. THEORETICAL ANALYSES

Young's modulus was calculated from the deformation data using a previously described theoretical model (Scott *et al.* 2004). For a hydrogel or epidermis suspended around its outer edge (figure 3), the total displacement that the indenter is lowered (δ) is equal to the sum of the depth of penetration into the hydrogel and the vertical deformation displacement of the hydrogel:

$$\delta = \left(\frac{9F^2(1-\nu^2)^2}{16RE^2} \right)^{1/3} + \frac{3Fa^2(1-\nu^2)}{4\pi Eh^3}, \quad (3.1)$$

where E is Young's modulus; F is the force applied to the tissue or hydrogel by the indenter; R is the radius of the indenter tip; a is the radius of the tissue or hydrogel sample inside the sample holder; h is the thickness; and ν is the Poisson ratio. For large deformation, stretching would also have to be taken into consideration (Liu & Wan 2008). As mentioned in §2.1, the values of a and R are 5.5 and 0.19 mm, respectively. From this equation, Young's modulus was calculated using MATLAB software (MathWorks, USA). The force can be reasonably assumed as a point loading, since the radius of the tip edge is small compared with the sample dimension ($R/a < 0.035$; Ju *et al.* 2004). For samples of thickness 0.5–0.8 mm and the total displacement (δ) not more than 1 mm, the influence of stretching on the deformation behaviour should be minimal (Liu & Wan 2008).

Two theoretical models were used to examine the relaxation behaviour of the hydrogels during experiments. The three-parameter standard linear model and five-parameter Maxwell–Weichert model were both used to describe the viscoelastic relaxation response under a constant strain. For a five-parameter Maxwell–Weichert model, which consists of a single spring and

two Maxwell elements in parallel, the total stress, $\sigma(t)$, equals the sum of the stresses applied to the spring and the Maxwell elements

$$\sigma(t) = \sigma_0 + \sigma_1 + \sigma_2, \quad (3.2)$$

where σ_0 is the stress applied to the spring and σ_1 and σ_2 are the stresses applied to each Maxwell element and whose values can be described as

$$\sigma_0 = \varepsilon E_0, \quad (3.3)$$

$$\sigma_1 = \varepsilon E_1 \exp\left(\frac{-E_1 t}{\eta_1}\right) \quad (3.4)$$

and

$$\sigma_2 = \varepsilon E_2 \exp\left(\frac{-E_2 t}{\eta_2}\right), \quad (3.5)$$

where η refers to the dashpot viscosity. By substituting equations (3.3)–(3.5) into equation (3.2), the stress relaxation function $g(t)$, which equates to $\sigma(t)/\sigma(0)$, can be described as

$$g(t) = A_0 + A_1 \exp\left(\frac{-t}{\tau_1}\right) + A_2 \exp\left(\frac{-t}{\tau_2}\right), \quad (3.6)$$

where A_0 , A_1 and A_2 represent the strain-dependent amplitudes,

$$A_0 = \frac{E_0}{(E_0 + E_1 + E_2)}, \quad (3.7)$$

$$A_1 = \frac{E_1}{(E_0 + E_1 + E_2)} \quad (3.8)$$

and

$$A_2 = \frac{E_2}{(E_0 + E_1 + E_2)}, \quad (3.9)$$

and τ_1 and τ_2 represent strain-dependent time constants,

$$\tau_1 = \frac{\eta_1}{E_1} \quad (3.10)$$

and

$$\tau_2 = \frac{\eta_2}{E_2}. \quad (3.11)$$

For the standard linear model, the stress relaxation function is written as

$$g(t) = A_0 + A_1 \exp\left(\frac{-t}{\tau_1}\right). \quad (3.12)$$

The values for A and τ were determined using nonlinear regression analysis for both relaxation models.

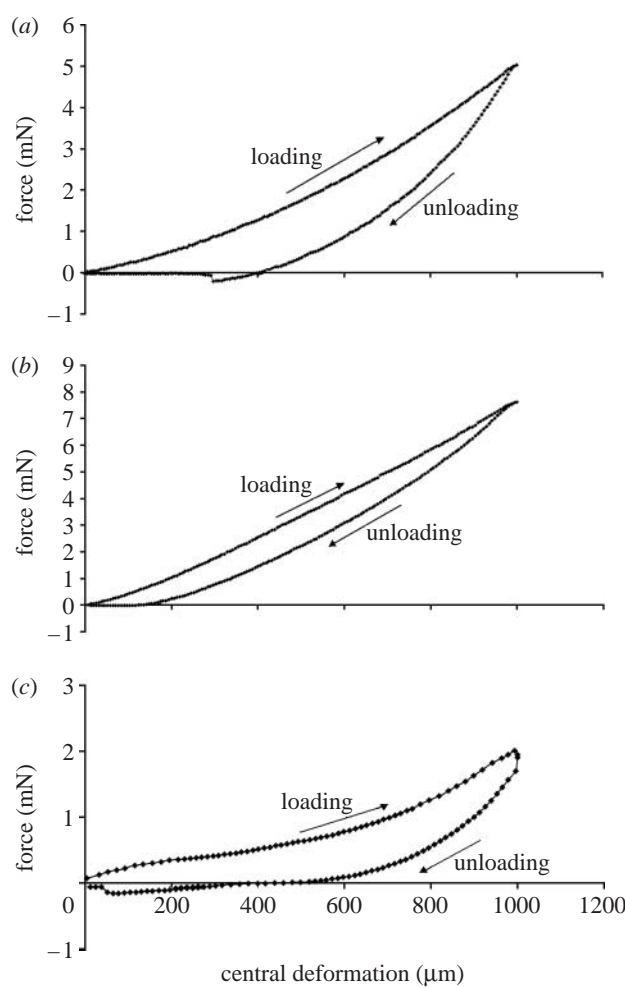


Figure 4. Loading–unloading depth sensing indentation data for a (a) 2% alginate hydrogel membrane, (b) 2% agarose hydrogel membrane and (c) chicken epidermis membrane.

4. RESULTS AND DISCUSSION

4.1. Young's moduli of membranes

Force–displacement curves for a 2 per cent (w/v) alginate, 2 per cent (w/v) agarose hydrogel membrane and a chicken epidermis membrane deflected to a central displacement of 1000 μm are shown (figure 4). It can be seen that the loading and unloading curves did not match. This type of behaviour, referred to as hysteresis, is common in viscoelastic materials and is the result of energy dissipation, fluid diffusion and polymer molecular realignment during loading. The loading–unloading curves appear less linear for alginate hydrogels than agarose hydrogels and there was a more significant difference between the loading and unloading curves for alginate. This suggests that alginate has nonlinear viscoelastic characteristics while agarose has more linear elastic characteristics. This type of mechanical behaviour agrees with the findings from previous publications (Bonn *et al.* 1998; Ahearne *et al.* 2005; Zhang *et al.* 2005). It was also found for some of the alginate hydrogels and the epidermis membranes that the force became negative for a short period during unloading. This can be explained by adhesion forces between the indenter and the hydrogel causing the indenter to adhere onto the hydrogel while unloading

(Gupta *et al.* 2007). The examination of the indenter after testing showed no residual material sticking to it. A small amount of olive oil was applied to the indenter to see if it would reduce the attraction between the indenter and the alginate, but this has no significant influence on the overall results.

Several loading and unloading cycles were recorded for individual samples. It was noticeable that different loading–unloading cycles on the same sample did not match although later loading–unloading cycles appeared to match much more closely than earlier cycles. It can be seen from figure 5a that for a 2 per cent alginate hydrogel, after the first cycle an increase in force was only detected after the indenter has been lowered by over 200 μm . This would suggest that plastic deformation of the alginate hydrogels had occurred in addition to elastic and viscoelastic deformation. Hydrogels such as agarose and alginate consist of a network of polymer chains swollen in solution. When a strain is applied to the hydrogel, fluid is pushed through the pores in the polymer network and the polymer chains are realigned. As the strain is increased, the ability of fluid to pass through pores is reduced and the polymer chains stiffen. The polymer network provides the elastic and plastic characteristics of the hydrogels while the solution provides the viscous characteristics. Plastic deformation, in addition to the viscous properties of the hydrogel, prevented the hydrogel from fully returning to its original shape. There was also a small decrease in the amount of force required to bend the hydrogel with each cycle. This decrease in force was reduced with each cycle until there was no functional force decrease detectable. This phenomenon is common in biological materials (Fung 1993) and is the combination of the realignment of polymer molecules and fluid movement within the sample. The loading–unloading cycles for agarose (figure 5b) appeared to match each other more closely than for alginate.

The loading–unloading behaviours of chicken epidermis were also examined (figure 5c). These tests were done to show how MSP can be applied to real biological tissues in addition to hydrogel membranes. The loading–unloading data were considerably different from the hydrogels since the epidermis had more nonlinear behaviour. This is not surprising because structurally the epidermis would differ from the hydrogels as it would contain cells, fibres and extracellular matrix proteins, which would affect its mechanical behaviour. It was found that there was a larger difference between the loading and unloading curves for these samples when compared with the hydrogels and that the amount of force required to deflect the samples was less than that for the hydrogels. The viscoelastic, nonlinear behaviour of the epidermis samples makes it difficult to calculate a modulus value accurately for the tissue. When the modulus was calculated for different deformation displacements, it was found that the modulus varied between 15 and 60 kPa (figure 6). These results fall within results from previous examinations of skin mechanics, which vary considerably with moduli being quoted between 12.5 kPa and 20 MPa (Paillet-Mattei *et al.* 2008). In addition to the nonlinear nature of the tissue, the

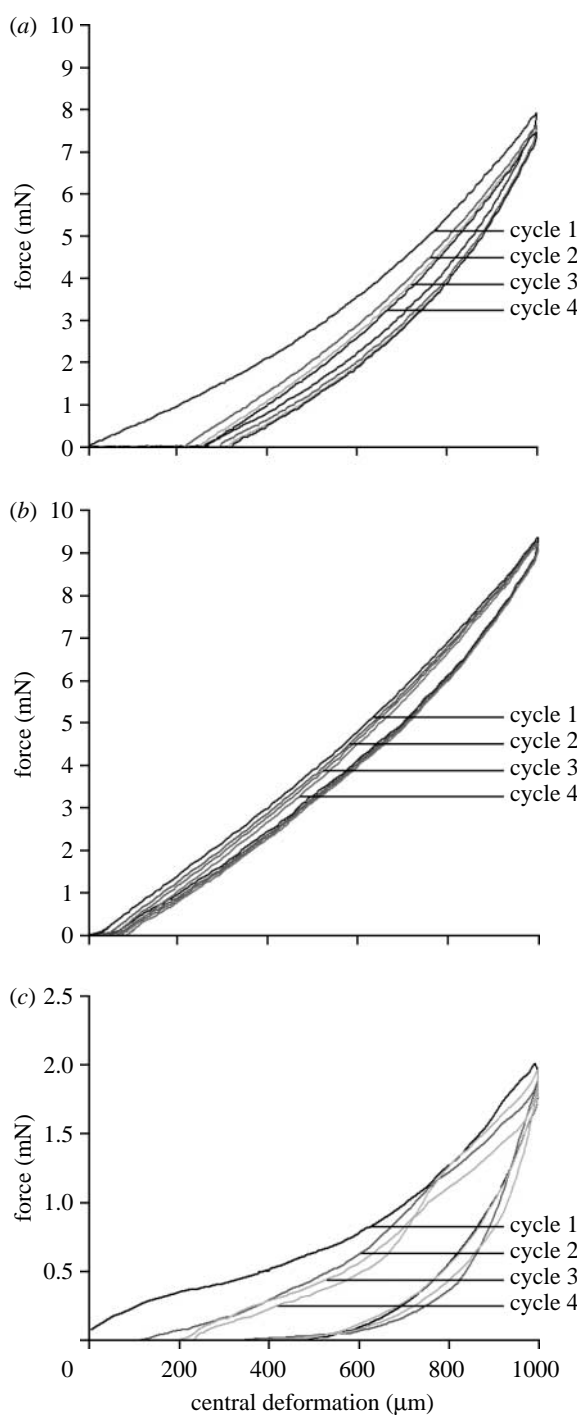


Figure 5. Loading–unloading cycles for a (a) 2% alginate hydrogel membrane, (b) 2% agarose hydrogel membrane and (c) chicken epidermis membrane (including sequential cycle number).

variation in moduli is dependent on the location from where the sample is taken, the mechanical characterization technique, the strain applied to the sample and the intrinsic strain prior to measurement. Intrinsic strain is particularly important as skin is normally in tension, which is lost once it has been removed for testing. A more in-depth study of epidermis and skin using the MSP should provide useful data on the mechanical properties of these tissues in the future.

Young's moduli of agarose hydrogels of different concentrations when the indenter was lowered 1000 μm are displayed (figure 7). Agarose was preferred to

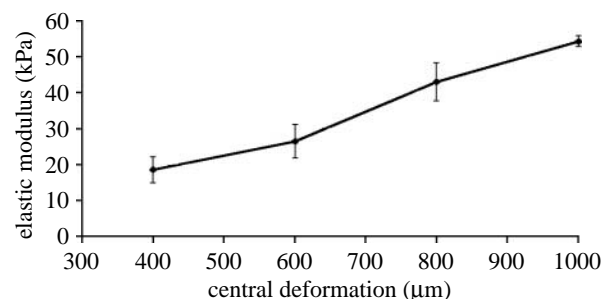


Figure 6. Variation in elastic modulus of chicken epidermis with central deformation.

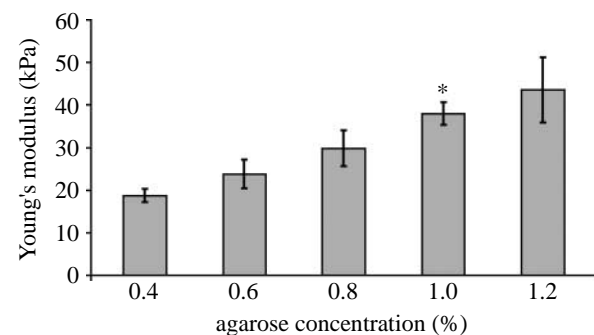


Figure 7. Young's modulus of agarose hydrogels measured by depth sensing microindentation (\pm s.e., $n=4$). Asterisk represents a significant difference with a 95% CI over the previous concentration determined using a one-way ANOVA Tukey's test.

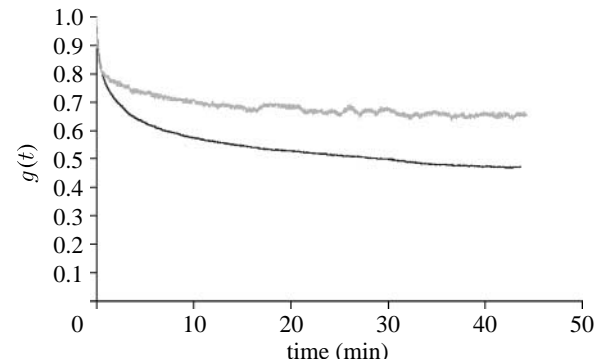


Figure 8. Stress relaxation function $g(t)$ calculated based on normalized relaxation data for a 2% alginate (black curve) and a 1% agarose (grey curve) hydrogel indented to 1000 μm .

alginate for calculating Young's modulus since it had a more linear elastic response to indentation. Young's modulus of alginate hydrogels varies in the literature with a range between 1 and 100 kPa (Kuo & Ma 2001; Awad *et al.* 2004; Drury *et al.* 2004). A nonlinear loading curve would result in the values for Young's modulus becoming dependent on the bending depth. It can be seen that there was an almost linear increase in Young's modulus with agarose concentration. Simple regression analysis was used to confirm the linearity of Young's modulus with agarose concentration between 0.4 and 1.2 per cent with a coefficient of determination (R^2) equal to 0.9935. The standard deviation bars show a high degree of repeatability in measuring different agarose hydrogels with the same concentration.

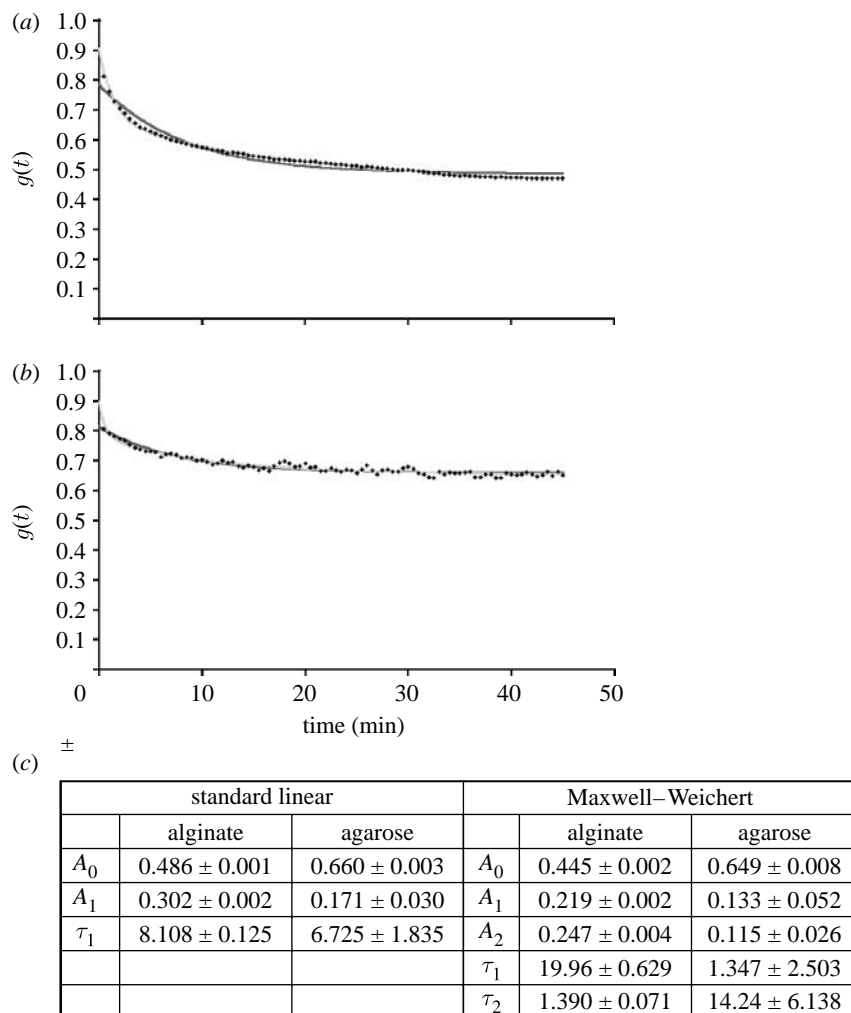


Figure 9. Actual and theoretical model normalized force data for (a) a 2% alginate and (b) a 1% agarose hydrogel at a constant indentation of 1000 μm . Diamonds, experimental data; black curve, standard linear model; grey curve, Maxwell-Weichert model.

Interestingly, when the same hydrogel was measured several times, the standard deviation was further reduced, i.e. for 0.5 per cent agarose hydrogel indented to 1000 μm four times, $E = 20.9 \pm 0.7 \text{ kPa}$.

The values obtained for Young's modulus of agarose were approximately two to three times higher than those found using our previous spherical indentation technique (Ahearne *et al.* 2005). Different mechanical models were used to describe each deformation, i.e. large deformation model with Mooney constitutive equations being used for the spherical indentation and a point load-bending model with linear elasticity for MSP. The deformation behaviour is very different in the two approaches, where stretching is dominant over bending in the large deformation model while bending is dominant over stretching in small deformation models as that used here (Liu & Wan 2008). The size and volume of the hydrogels also differed between the two approaches. In addition, despite agarose having a more elastic nature than alginate, it still exhibits nonlinear viscoelastic characteristics that can cause a problem when calculating Young's modulus from the loading-unloading curves. Variations such as these have previously been shown when examining a common material using different techniques (Korhonen *et al.* 2002; Harley *et al.* 2007). Despite this, the values

obtained for 1 per cent agarose by this method appear to resemble those found by Bonn *et al.* (1998) using three-point bending and Nyland & Maughan (2000) using atomic force microscopy, where only small deformations were involved in their mechanical models.

4.2. Stress relaxation of membranes

Normalized force relaxation data were collected for agarose and alginate hydrogels. The samples were deflected to a central displacement depth of 1000 μm , which was maintained for 45 min. For times longer than 45 min, dehydration of the hydrogel would affect the measurement readings. The weight of the hydrogels was reduced by only 1–1.5 per cent after 45 min out of water, which suggests that a limited amount of dehydration has taken place. Both agarose and alginate appeared to exhibit relaxation behaviour consistent with viscoelastic materials (figure 8). The amount of force required to maintain the deflection displacement was reduced over time. The normalized force initially decreased quickly but then slowed until reaching a plateau. Alginate appeared to demonstrate a greater relaxation response than agarose, which suggests it is more viscoelastic than agarose, which has more elastic characteristics.

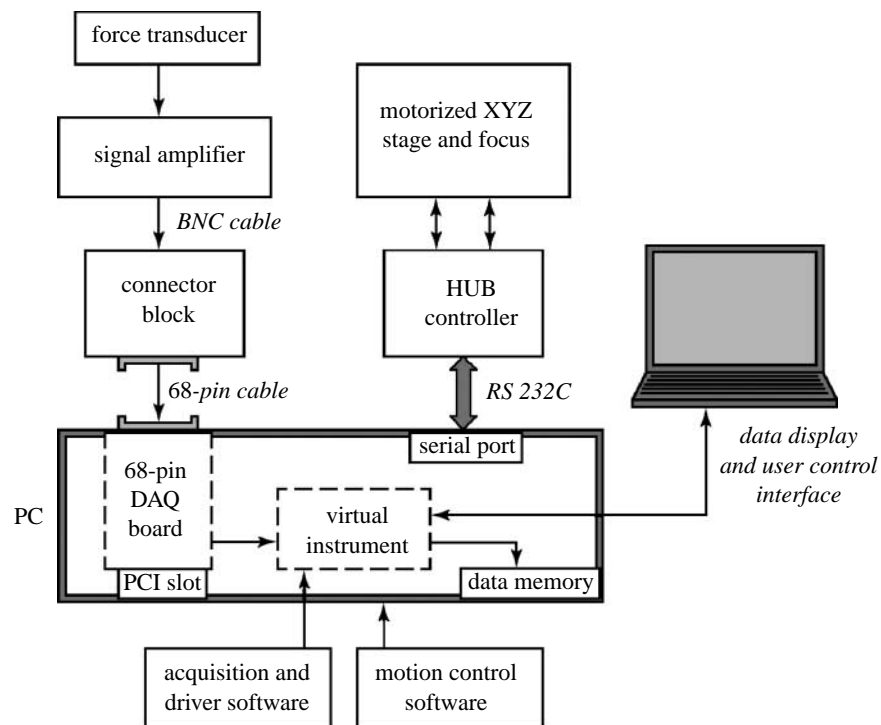


Figure 10. A simplified block diagram of the system showing the interconnections between instrumentation, DAQ and control interface.

Nonlinear regression analysis, performed using XLSTAT (Addinsoft, USA), was used to determine the ability of the three-parameter standard linear model and five-parameter Maxwell–Weichert model to describe the hydrogels' relaxation responses to the deformation applied by MSP. Both models appear to show a high degree of correlation between the actual data and the theoretical model data (figure 9). Coefficients of determination (R^2) for both the models were found for both agarose and alginate hydrogels. The values for R^2 for agarose and alginate hydrogels were found to be greater than 0.9 using the standard linear model and greater than 0.95 for the Maxwell–Weichert model. This would appear to suggest that the five-parameter Maxwell–Weichert model is capable of providing a more accurate representation of the relaxation response than the standard linear model. This is to be expected as increasing the number of parameters or elements should improve the accuracy of the model. The drawback of increasing the number of parameters includes longer times that are required for calculation to be performed and the physical meaning of the parameters may be lost.

5. CONCLUSIONS

The MSP method has been applied to examine the mechanical and viscoelastic characteristics of various biomimetic and biological membranes and the results have been demonstrated to be satisfactory. Incorporated with simple analyses, the new instrument has been shown to be capable of determining quantitatively viscoelastic and mechanical properties based on experimental data of loading–unloading and stress relaxation curves. The

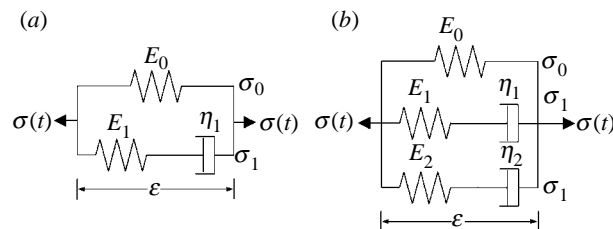


Figure 11. Schematic of the (a) three-parameter standard linear model and (b) five-parameter Maxwell–Weichert model.

instrument has potential for testing other soft biological materials, such as human skin.

We are grateful for the financial support from North Staffordshire R&D consortium.

APPENDIX A

A detailed description of the interconnections among the instrumentation, DAQ and control is shown in figure 10.

The three-parameter standard linear model and five-parameter Maxwell–Weichert model were both used to describe the viscoelastic relaxation response under a constant strain (figure 11).

REFERENCES

Ahearne, M., Yang, Y., El Haj, A. J., Then, K. Y. & Liu, K. K. 2005 Characterizing the viscoelastic properties of thin hydrogel-based constructs for tissue engineering applications. *J. R. Soc. Interface* **2**, 455–463. (doi:10.1098/rsif.2005.0065)

Awad, H. A., Quinn Wickham, M., Leddy, H. A., Gimble, J. M. & Guilak, F. 2004 Chondrogenic differentiation of

adipose-derived adult stem cells in agarose, alginate and gelatin scaffolds. *Biomaterials* **25**, 3211–3222. (doi:10.1016/j.biomaterials.2003.10.045)

Bonn, D., Kellay, H., Prochnow, M., Ben-Djemaa, K. & Meunier, J. 1998 Delayed fracture of an inhomogeneous soft solid. *Science* **280**, 265–267. (doi:10.1126/science.280.5361.265)

Callister, W. D. 1994 *Materials science and engineering, an introduction*, 3rd edn. New York, NY: Wiley.

Drury, J. L., Dennis, R. G. & Mooney, D. J. 2004 The tensile properties of alginate hydrogels. *Biomaterials* **25**, 3187–3199. (doi:10.1016/j.biomaterials.2003.10.002)

Espinosa, H. D., Prorok, B. C. & Fischer, M. 2003 A methodology for determining mechanical properties of freestanding thin films and MEMS materials. *J. Mech. Phys. Solids* **51**, 47–67. (doi:10.1016/S0022-5096(02)00062-5)

Fung, Y. C. 1993 *Biomechanics: mechanical properties of living tissues*, 2nd edn. New York, NY: Springer.

Gupta, S., Carrillo, F., Li, C., Pruitt, L. & Puttlitz, C. 2007 Adhesive forces significantly affect elastic modulus determination of soft polymeric materials in nanoindentation. *Mater. Lett.* **61**, 448–451. (doi:10.1016/j.matlet.2006.04.078)

Harley, B. A., Leung, J. H., Silva, E. C. C. M. & Gibson, L. J. 2007 Mechanical characterization of collagen-glycosaminoglycan scaffolds. *Acta Biomater.* **3**, 463–474. (doi:10.1016/j.actbio.2006.12.009)

Ju, B. F., Wan, K. T. & Liu, K. K. 2004 Indentation of a square elastomeric thin film by a flat-ended cylindrical punch in the presence of long-range intersurface forces. *J. Appl. Phys.* **96**, 6159–6163. (doi:10.1063/1.1812822)

Khoo, H. S. 2003 Characterization of mechanical properties of microfabricated film. MPhil theses, School of Mechanical and Production Engineering, Nanyang Technological University.

Korhonen, R. K., Laasanen, M. S., Toyras, J., Rieppo, J., Hirvonen, J., Helminen, H. J. & Jurvelin, J. S. 2002 Comparison of the equilibrium response of articular cartilage in unconfined compression, confined compression and indentation. *J. Biomech.* **35**, 903–909. (doi:10.1016/S0021-9290(02)00052-0)

Kuo, C. K. & Ma, P. X. 2001 Ionically crosslinked alginate hydrogels as scaffolds for tissue engineering: part 1. Structure, gelation rate and mechanical properties. *Biomaterials* **22**, 511–521. (doi:10.1016/S0142-9612(00)00201-5)

Liu, K. K. & Ju, B. F. 2001 A novel technique for mechanical characterization of thin elastomeric membrane. *J. Phys. D: Appl. Phys.* **34**, L91–L94.

Liu, K.-K. & Wan, K.-T. 2008 Multi-scale mechanical characterization of a freestanding polymer film using indentation. *Int. J. Mater. Res.* **99**, 862–864. (doi:10.3139/146.101712)

Liu, K. K., Khoo, H. S. & Tseng, F. G. 2004 *In situ* mechanical characterization of square microfabricated elastomeric membranes using an improved microindentation. *Rev. Sci. Instrum.* **75**, 524–531. (doi:10.1063/1.1638894)

Lu, S., Dikin, D. A., Zhang, S. & Fisher, F. T. 2004 Realization of nanoscale resolution with a micromachined thermally actuated stage. *Rev. Sci. Instrum.* **75**, 2154–2162. (doi:10.1063/1.1710703)

Menciassi, A., Scalari, G., Eisinberg, A., Anticoli, C., Francabandiera, P., Carrozza, M. C. & Dario, P. 2001 An instrumented probe for mechanical characterization of soft tissues. *Biomed. Microdevices* **3**, 149–156. (doi:10.1023/A:1011454427384)

Nyland, L. R. & Maughan, D. W. 2000 Morphology and transverse stiffness of *Drosophila* myofibrils measured by atomic force microscopy. *Biophys. J.* **78**, 1490–1497. (doi:10.1016/S0006-3495(00)76702-6)

Pailler-Mattei, C., Bec, S. & Zahouani, H. 2008 *In vivo* measurements of the elastic mechanical properties of human skin by indentation tests. *Med. Eng. Phys.* **30**, 599–606. (doi:10.1016/j.medengphy.2007.06.011)

Ratner, B. D., Hoffman, A. S., Schoen, F. J. & Lemons, J. E. 1996 *An introduction to materials in medicine*. New York, NY: Academic Press.

Scott, O. N., Begley, M. R., Komaragiri, U. & Mackin, T. J. 2004 Indentation of freestanding circular elastomer films using spherical indenters. *Acta Mater.* **52**, 4877–4885. (doi:10.1016/j.actamat.2004.06.043)

Zhang, J., Daubert, C. R. & Foegeding, E. A. 2005 Fracture analysis of alginate gels. *J. Food Sci.* **70**, e425–e431. (doi:10.1111/j.1365-2621.2005.tb11471.x)